Lasers in Manufacturing Conference 2015

3D laser micro-machining for targets manufacturing

Bourdenet R.*, Geoffray I., Chicanne C., Theobald M.

CEA, Centre de Valduc, 21120 Is Sur Tille, France

Abstract

High power experiments require complex targets that include various geometries and materials. Laser micro-machining processes offer reliable and accurate solutions, able to fulfill demanding specifications. This paper gives examples of recent developments in 3D laser micro-machining of targets components, involving either UV nanosecond pulses (excimer laser) or ultrashort pulses (Ti:Sa femtosecond laser).

Keywords: femtosecond laser ; excimer laser ; pulsed UV laser ; micro-machining ; targets

1. Motivation / State of the Art

CEA designs, studies and manufactures targets in order to achieve experiments on high energy laser (Laser MegaJoule). A target is a centimetric complex experimental object that is usually composed of a gold outer component (hohlraum) containing a wide range of materials (metals, foams, plastics …). The hohlraum is composed of a high-Z material and converts the focused beams into X-rays radiation that interact with a given sample (indirect drive scheme). Different physical phenomena are currently studied (laser-plasma interactions, radiation transport, high energy density physics,…).
Materials that compose targets are often thin (thickness often below 0.1 mm) and fragile. Their manufacture requires high-level micro-technology means [1].

Among those technologies, 3D laser micro-machining processes combining accuracy and repeatability are currently being developed. This paper presents two examples:

- The first one shows how submillimetric and low-density microspheres can be laser-machined. Such

* Corresponding author: remy.bourdenet@cea.fr

components synthesized with a material (silica aerogel) that combines high-Z elements and quite low densities (0.3 $g.cm^{-3}$). The ability to make these aerogels into spheres with severe specifications is important for the study of implosion phenomena [2].

- The second example deals with controlled mathematical functions (sine curve in that case) that are laser-engraved onto polymer capsules [3]. The defect is made purposely on the outer surface of capsules and allows the study of hydrodynamic modes growth (that occurs along the implosion process).

1.1. Silica aerogel machining

Silica aerogel is a low density (< 300 $mg.cm^{-3}$) inorganic nanostructured material. The home-made synthesis protocol of silica aerogels requires sol-gel polymerization of silicon alkoxide followed by a supercritical drying.
As a result, the material is transparent and shows small pore size. It is usually quite brittle and not easily machinable by conventional means due to void that represents up to 95% of the volume. Thanks the ultra-precision machining (milling) [4], targets components are currently manufactured but some geometries are difficult to be implemented.
So laser processes are attractive alternatives because they feature small interaction volume and a low induced mechanical stress. However, laser technologies have to deal with the low absorbance of this material in the visible and near-infrared range (see fig 1).

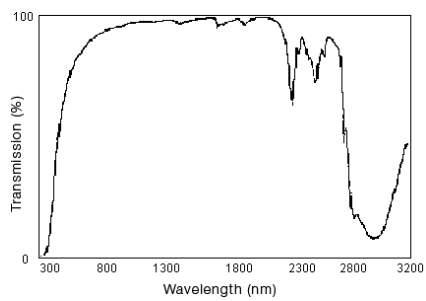

Fig. 1. Silica aerogel absorbance [3]

Considering the graph, an ArF excimer laser (emitting at 193 nm) is an appropriate source: (i) the absorption is high (pretty below the cut-off wavelength), (ii) the energy carried by UV photons (6.4 eV) is higher than the bonds dissociation energy (e.g. 4.7 eV for O-Si), leading to an efficient material decomposition. In that case, ablation is mainly driven by a photochemical process, but photothermal effects can remain.

Another solution involves a femtosecond laser emitting in the near-infrared (800 nm). With a short focal length, associated to ultra-short pulses, high peak power can overcome the high bandgap of dielectric materials. Indeed, an efficient absorption of this transparent material can be achieved from nonlinear effects such as multiphoton absorption and avalanche ionization [5, 6]. Another advantage is a reduced HAZ and the absence of thermal shock cracking in any of the surrounding material (suitable for brittle-materials machining). In addition, all regions throughout the laser beam profile with sufficient intensity for multiphoton ionization will be removed, resulting in fine control of the position of material removal.

1.2. Polymer capsule machining

Germanium or silicon doped amorphous hydrogenated carbon (a-C:H or CHx) is synthesized by glow discharge polymerization (GDP) coating on a depolymerizable mandrel [7]. This process leads to sub-millimetric free-standing ablator capsules. The following step consists in engraving one hemisphere (the other remaining blank).

For this last step, a laser process has been chosen due to its reliability (that allows getting this specific geometry).
In addition, a process based on femtosecond pulses offers several advantages:

- The efficiency of ablation process, especially for polymer materials,
- The small achievable spot size (a few micrometers - near the diffraction limit), leading to low tool radius and thus avoiding a geometric distortion of the sine function.
- The accurate beam spotting system that equipped the femtosecond laser workstation. Its resolution and magnification (x500 combining optical device and digital processing) lead to an accurate positioning of capsules under the beam spot. This criterion is important to reach the required tight specifications described below.

2. The laser workstations

The excimer workstation includes a Lambda-Physik laser (CompEx) delivering 450 mJ at 193 nm. The pulse width is 20 ns, and the repetition rate is tunable between 1 Hz and 50 Hz. The associated optical bench is designed in mask-projection configuration, where the mask is imaged on the sample with a demagnification factor of 8 or 15 (according to the chosen optics). This way, the spatial shape of the beam can be adapted to the requested machining geometry, and is devoid of aberration or diffraction effects. Masks are manufactured by laser micromachining or by electro-erosion techniques.

In the femtosecond laser workstation, a commercial Ti:sapphire laser system (Quantronix / Integra-C) is used; this laser delivers an energy up to 2 mJ at 800 nm, with a repetition rate of 1kHz. The pulse width is lower than 150 fs. The output beam is Gaussian with a quality factor (M^2) lower than 1.4. An external SHG device can be added to get a wavelength of 400 nm with conversion efficiency over 30%.
The laser beam is focused with an achromatic doublet. According to the chosen focal length, beam diameter at the focal plane is in range 3 µm – 20 µm. The associated Rayleigh distance is low (generally lower than 200 µm) but fits into the common sample thicknesses.

The two workstations include four-axis systems (three linear stages and a rotary stage) that move the samples under the laser beam. The stages repeatability and accuracy are better than 1 µm.

3. Aerogel microspheres manufacturing

The study was performed with silica aerogel centimetric samples that are synthetized in densities as low as 200 $mg.cm^{-3}$ and 300 $mg.cm^{-3}$. The aim was to shape such massive samples into small spheres featuring a diameter of 360 µm and 490 µm.

Excimer and femtosecond-laser based processes were developed. In both cases, laser and motion parameters were refined to optimize the shells geometrical defects (roundness) as well as the surface quality (arithmetical roughness).

3.1. Experimental

Developments included a generic multi-step protocol, with (a) a first step where the material was roughly machined into a cylinder, (b) a rough machining of a sphere supported by a little stalk, (c) a finishing step (layer by layer machining cycles) up to obtain the final diameter supported by a thinner stalk, (d) the final step where the stalk was progressively cut off (see fig 2).

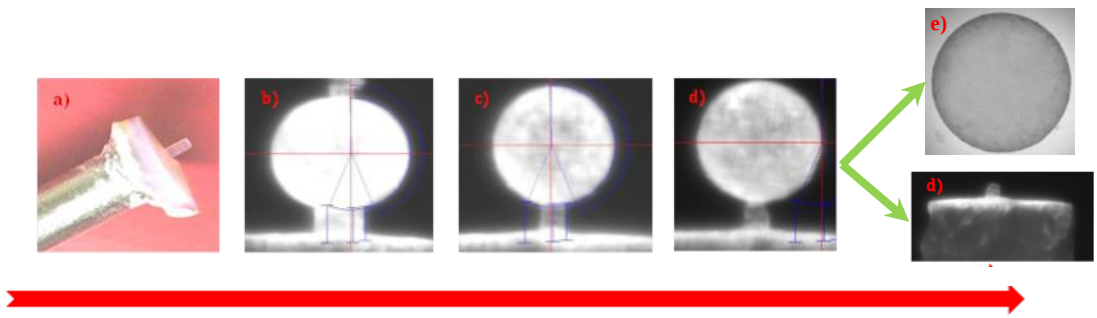

Fig. 2. Micro-balls manufacturing steps : a) cylinder shaping b) Rough ball shaping c) Ball finishing and d) stalk cutting-off e) foamball

Studies involving ultra-short pulses (Ti:Sa laser) were realized at the fundamental wavelength. The longitudinal beam profile was adjusted to work with a reduced ablation volume. Thus a 60 mm focal length combined with a beam expander (magnification x 2) was used to obtain a 5 µm beam spot, with a corresponding Rayleigh distance of about 20 µm. The pulse energy was adjusted to be just over the threshold, getting the material ablation with reduced collateral damages. The best compromise led to a fluence level of about 80 J/cm^2.

The sample motion was programed to get circular X,Y move while turning around Theta axis. Refined parameters were mainly linked to motion and geometrical considerations:

- The rotary speed / X,Y axis speeds couple: to reduce residual streaks that could appear on the microsphere surface,
- The stalk diameter and the spot size: to limit the stalk's cutting default (see fig.2d)) and avoid a local geometric effect (flat surface),
- The beam spotting criteria, which influenced directly the spheres roundness, as shown in figure 3.

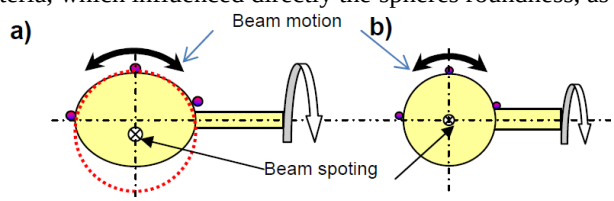

Fig. 3. Roundness error due to beam spotting

Studies involving the excimer laser beam were realized with a demagnification factor of 15 for the mask-projection system (leading to higher fluences in the image focal plane). The specific mask is shown in fig 4. It

included a half-moon shape with a bottom rectangular part (the stalk). It was manufactured with margins lower than ± 0.02 mm: considering the optical demagnification of the system, the error on the diameter was lower than 0.002 mm.

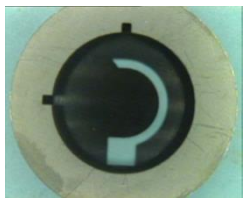

Fig. 4. Foamball mask

The mask was positioned on a manual rotary stage and then aligned with X and Y linear axis. As for the femtosecond study, the fluence level was adjusted near the ablation threshold, at a value of about 9 J/cm^2. The following parameters were refined according to the materials densities: sample motion speed, pulse energy, mask's aperture.

3.2. Results and Discussion

The results are presented in table 1 and figure 5.

Table 1. Spheres results (silica aerogels - 300 mg.cm^{-3})

Manufacturing tolerances	ArF laser	Ti:Sa laser
Sphere diameter	± 0.02 mm	± 0.01 mm
Out of round	0.002 mm	< 0.002 mm
Arithmetic Roughness	0.005 mm	< 0.002 mm
Local defaults (max size) (stalk removing)	0.06 mm diameter and 0.005 mm high	0.03 mm diameter and 0.006 mm high

Uncertainties in measurements: ± 0.01 nm for the roughness and ± 0.001 mm for the other data

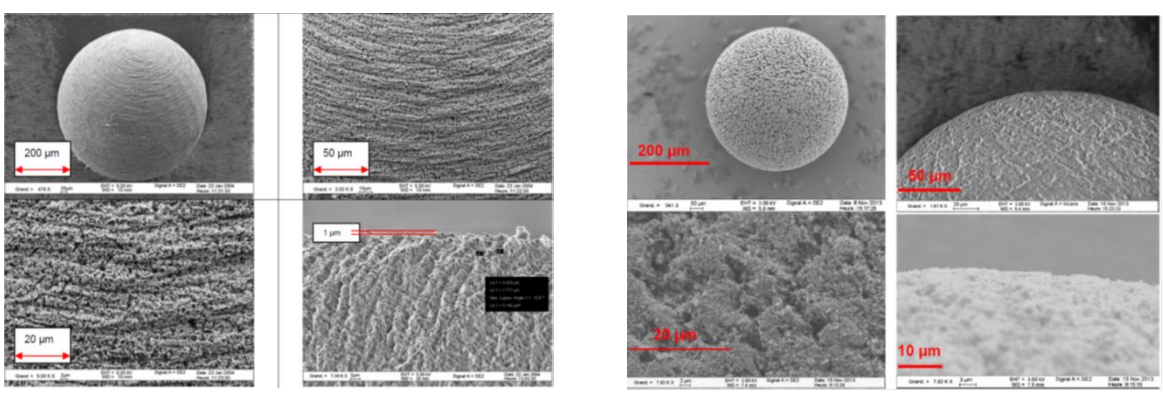

Fig. 5. SEM spheres images a) Excimer laser technique b) femtosecond laser process (silica aerogels - 300 mg.cm^{-3})

Both excimer and femtosecond techniques were successful to shape silica aerogel into spheres. However, a deeper analysis of results highlights differences between both processes:

- Manufacturing tolerances were tighter (± 10 µm with Ti:Sa laser and ± 20 µm with ArF laser) with a femtosecond laser because the programmed diameter has been adjusting along the machining process, up to reach the specified value (in-situ dimensional measurements). This was not allowed by excimer laser, where the diameter was fixed by the mask shape.

- Out of rounds as low as 2 µm were obtained in both cases, proving that the beam spotting adjustment was accurate enough on the two workstations. The local defect induced by the stalk tended to be lower (0.03 mm diameter and 0.006 mm high) with the femtosecond process due to a smaller radius tool on this area.

- Surface seemed more homogeneous with a femtosecond laser. Indeed, SEM images (see fig 5) showed streaks on the sphere manufactured by excimer laser, which were not visible on those obtained by femtosecond laser. This was in coherence with the measured roughness, which was half in the case of femtosecond laser machining. Such differences could actually come from the temporal regime of the laser source. In ultra-short pulse regime, the various chemical elements (mainly Si and O, but also C and H) show a similar ablation threshold and are efficiently removed [8]. By comparison, a nanosecond regime leads to an ablation process driven by the linear absorption: a species-dependent and less homogeneous material removal could be obtained in that case.

- Another comment concerns the material density that strongly influenced the suitability of excimer laser machining. If the excimer process was efficient for density of 300 $mg.cm^{-3}$, it wasn't possible to manufacture capsules at a density as low as 200 $mg.cm^{-3}$ (see fig 6). The low absorption in the UV range was actually too low and inadequate to reach a stable and efficient ablation process. One option was to increase the pulse energy, but it had a detrimental effect on the sample (with mechanical effects breaking the stalk). The mask aperture has also been enlarged to increase the ablation area, without success. So excimer process was not suitable for the lowest densities, leading to an incompatibility of the requested fluence level and the sample geometry (fragile stalk). On the other hand, no effect of the density has been noted in the field of the femtosecond laser machining, due to the occurrence of a multiphoton absorption (as discussed below).

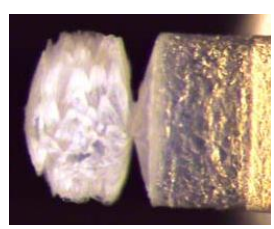

Fig. 6. Image of a machining test of 200 $mg.cm^{-3}$ aerogel silica by excimer ArF-laser

4. Capsules engraving

Ge:CHx or Si:CHx shells as involved in laser experiment show an inner diameter of 560 µm, for a 40µm-thick wall. The laser machining consisted in engraving sine profiles (period less than 100 µm and pk-pk amplitude of 4 µm) on one hemisphere. The modulation had to be centered on the capsule and buried under the surface from a constant and controlled depth (< 10 µm).

4.1. Experimental

The modulation was obtained by Ti:Sa femtosecond laser machining. Fundamental and frequency-doubled wavelengths were tested. Optical paths have been optimized to get small spot sizes at the focal plane (about 5 µm at 800 nm and 3 µm at 400 nm), leading to small tool radius.
The pulse energy has been refined to ablate while reduced thermal effects and material projection. Fluences about 12 J/cm^2 at 800 nm and 23 J/cm^2 at 400 nm seemed to be good compromises and have been chosen.

For the machining, the capsule was glued on a stalk and inserted into the rotary stage to be positioned at the focal plane. In order to warrant a regular burying depth, several adjustments have been required:

- The shell runout had to be minimized: the goal was avoiding X, Y or Z shifts between capsule and beam spot during the machining. A top runout defect of 2 µm was allowed.
- Beam spotting and sphere positioning had to be performed with an accuracy better than 2 µm.

These adjustments were critical because a global error higher than 6 µm could lead to detrimental effects (irregular burying depth, lacks of engraving).

These adjustments done, the capsule has been engraved by a succession of adjacent passes. The capsule has indeed been moved in the XY plane by describing a sine profile onto its outline, according to the following equations:

$$X = (R + 2a * \cos(\frac{2\pi * R * \alpha}{\lambda})) * \sin(\alpha)$$

$$Y = (R + 2a * \cos(\frac{2\pi * R * \alpha}{\lambda})) * \cos(\alpha)$$

With 2a=4 µm: peak to peak amplitude, λ=70 µm or 100 µm: period, R: capsule outer radius,
α : 0° to 120°.

Once the first arc of circle completed, the rotary turned by an angular pitch θ (see fig. 7). Motions have been repeated until the modulation covered one hemisphere (from 0° to 180 °).

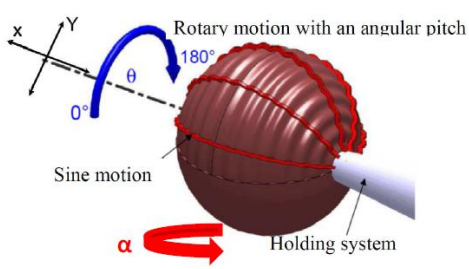

Fig. 7. Sketch of the engraving capsule process

4.2. Results and Discussion

The process allowed engraving an angular sector of 120° x 180°. To increase the machined area up to the pole (α>120°), a fifth stage should be necessary, but this equipment was not available on the laser workstation. On the other hand, the motion parameters were refined. For example, an angular pitch over 1° formed some flats on the machining area (due to a too large overlap between two adjacent passes).
Motion speed and angular pitch were optimized to get a process time short enough to keep the beam spot within 6 µm, as explained above. On the other hand, a too fast speed decreased manufacturing accuracy that was affected by acceleration and deceleration.

Results obtained with the frequency-doubled Ti:Sa laser are presented below.

As shown in table 2, fabrication tolerances (amplitude and wavelength of the sine function) were lower than ± 2 µm, within uncertainty measurements. Corresponding profiles were smooth (see fig. 8): the measured points (red) obtained after subtracting the sphere radius were closed to the theoretical sine profile (blue).
On the other hand, the machining area was free of thermal defects or debris to the surroundings (see fig. 9).

An average burying depth of 9 µm has been achieved. We noted a disparity along both 180° and 120° axis due to the process sensibility to the preliminary adjustments (runout and capsule positioning) that were the key parameters of this process.

Table 2. Results

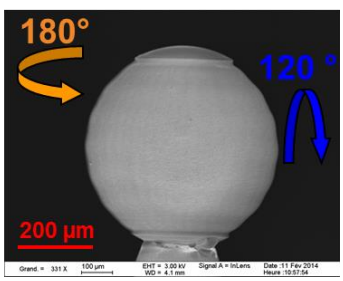

	Min	Max	Average
Amplitude (a)	1,7 µm	2.0 µm	1,9 µm
Wavelength 1 (70 µm)	69 µm	70 µm	70 µm
Wavelength 1 (100 µm)	99 µm	101 µm	100 µm
Burying depth	5 µm	14 µm	9 µm
Δ burying depth around120°	0 µm	7 µm	2 µm
Δ burying depth around180°	2 µm	5 µm	3 µm

Uncertainties in measurements: ± 0.5 µm for the amplitude, ± 1 µm for the burying depth and ± 5 µm for the wavelength.

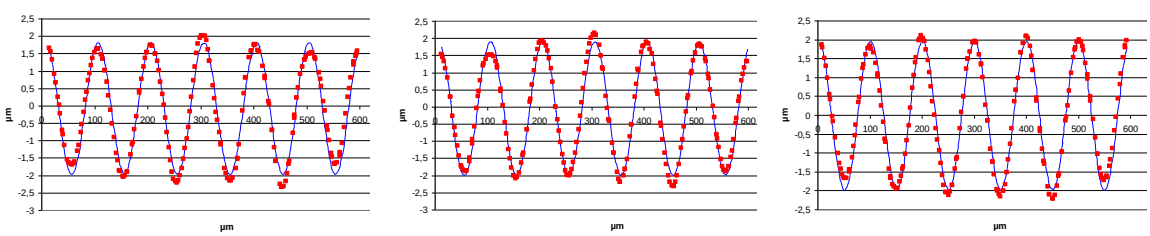

Fig. 8. Graphs of the sinusoidal modulation after removing the sphere radius profile from different angles (-45°, 0°, +45°)

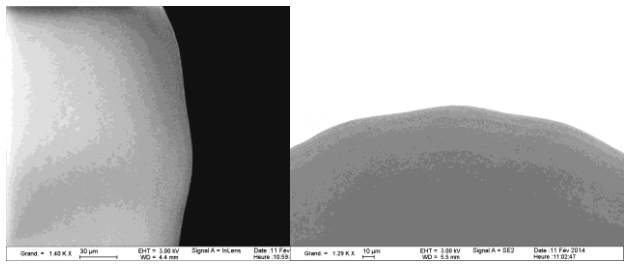

Fig. 9. SEM images of engraved capsule

For a wavelength of 800 nm, the material behavior was drastically different than in the UV range. In that case, a metallization of the engraved area has been noticed for Ge and Si (4% atom) doped CHx capsules (see fig 10). This phenomenon was not observable for a machining at 400 nm.
One assumption explaining this discrepancy is given below.

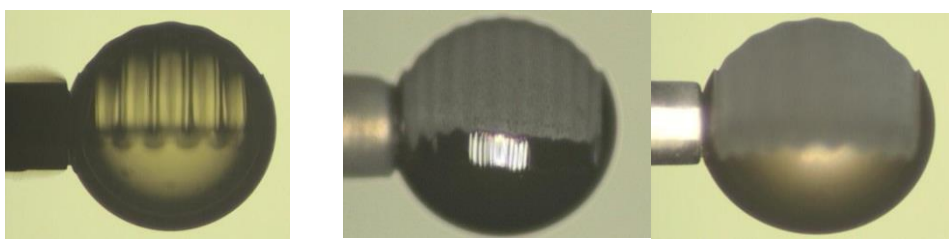

Fig. 10. Images of engraved capsules from left to right: CH Ge sphere engraving at 400 nm, CH Ge sphere engraving at 800 nm ,and CH Si sphere engraving at 800 nm

In the focalised volume, a multiphoton absorption followed by an ionization avalanche phenomenon was established at 400 nm and 800 nm. This process leads to a multi-modal panache of ablated material, that is composed of a first fast component (vaporisation of the outer material surface) followed by a slower component (nanometric and micrometric aggregates coming from a deeper volume). Dopant particles (Ge or Si, heavier than C and H) are ejected. But as the process is under ambiance, they slow down and coat onto the sphere [9].
In all cases, the capsule is machined tangentially, meaning that the surface is finally ablated by the extremely beam edge. In this area, the intensity decreases, probably to a value below the multiphoton interaction threshold.
For a wavelength of 400 nm, the energy carried by one photon (3.1 eV) is greater than dissociation energy of bounds like C-Ge (2.5 eV) or Ge-Ge (2 eV). Therefore, a photochemical effect could remain even in beam periphery, inducing the dopant (Ge or Si) removal along the ablation process by spatial overlapping of several adjacent pulses.
While at 800 nm, the photon energy (1.55 eV) is below the bounds dissociation energies, and the coated layer of dopant can't be removed, even with overlapped pulses. Further studies will be performed to confirm this assumption.

5. Conclusion

This paper shows the feasibility of 3D laser micromachining. Among the available means, the femtosecond laser technology is the most flexible. It allows shaping a large range of materials and therefore has become essential in the field of micro-targets manufacturing. As example, low density and brittle material like silica aerogel have been machined into spheres (diameter < 500 µm) with out of rounds as low as 2 µm. Plastic capsules have also been machined into specific geometry, like an sine function that was engraved with a high accuracy: pk-pk amplitude (4 µm) and wavelength (< 100 µm) were fulfilled with a top deviation of 1 µm. Developments are being continued to adapt this versatile technology to the future targets geometries and materials.

References

[1] Reneaume, B et al.: Overview on materials and technological developments for the LMJ cryogenic target assembly. Fusion sciences and technology, vol 59 (2011), 148-154

[2] M. Bono, D. Bennett,C. Castro, J. Satecher, J. Poco, B. Brown, H. Martz, N. Teslich, r. Hibbard, A. Hamza, P. Amendt, H. Robey, Fabrication of double shell targets with a glass inner capsule supported by SiO_2 aerogel for shots on the omega laser in 2006. Fusion science and technology, vol 51 (May 2007), 611-625

[3] K.A.D Obrey, F. Fierro, J. Martinez. Utilizing conventional machining tools with customized machining technique to manufacture multifaceted targets. Fusion science and technology, vol 63 (Marsh 2013), 247-251

[4] A. Soleimani Dorcheh , M.H. Abbasi. Silica aerogel; synthesis, properties and characterization Journal of material processing technology 199 (2008), 10-26

[5] X. Liu, D. Du, and G. Mourou, Laser Ablation and Micromachining with Ultrashort Laser Pulses IEEE JOURNAL OF QUANTUM ELECTRONICS, vol 33 (1997)

[6] K. Sugioka and Ya Cheng; Femtosecond laser three-dimensional micro- and nanofabrication APPLIED PHYSICS REVIEWS 1, 041303(2014)

[7] C. Chicanne, J. Bray, E. Peche, G. Legay, M. Theobald, O. Legaie, A. Ollagnier and E. Finot; Germanium doped CHx microshells for LMJ targets - Fusion science and technology, vol 59 (January 2011), 87-93

[8] I. Geoffray, A. Faivre, S. Bednarczyk, R. Bourdenet Laser micro-machining for high precision targets fabrication , Proceeding for Conference LIM 2009, 653-658

[9] Mark Stuart Bennett Darby, Thesis Femtosecond Pulsed Laser Deposition, UNIVERSITY OF SOUTHAMPTON FACULTY OF ENGINEERING, SCIENCE & MATHEMATICS January 2009